Explanations for the exceptional activity of Au nanostructures often include a direct role played by the support, such as at the perimeter of the Au-support interface (*7*, *9*, *28*, *29*). Our data show that the TiO_x support is crucial as a dispersant and a promoter of the Au overlayer, but that TiO_x itself cannot be directly involved in the bonding of O_2 or CO, because in the Au-(1×1) and -(1×3) structures, the Au overlayer precludes access to the Ti cation sites by the reactants. That an optimum reactivity is seen for the (1×3) Au structure strongly suggests that a combination of the first- and second-layer Au sites is necessary to promote reaction between CO and O_2. The interaction of the first-layer Au with Ti^{3+} of the support, yielding $Au^{\delta-}$, likely is crucial for activation of O_2 (*3*, *4*, *21–23*). CO, however, has been shown to adsorb strongly on the Au bilayer structure (*5*, *6*). For the more general case of Au/TiO_2, mono- and bilayer Au islands in the <4-nm diameter range form as a result of Au atoms nucleating initially at Ti^{3+} defect sites (*2*), then with the addition of more Au, evolve into Au bilayer islands stabilized by the bonding between the interfacial Au atoms and Ti^{3+} defects that accumulate at the Au-TiO_2 interface (*21–23*, *30*). The mono- and bilayer Au islands seen for Au on TiO_2(110) (*2*) have also been observed for Au supported on high-surface-area TiO_2 by Lupini and co-workers (*31*). These mono- and bilayer Au structures appear to be truncated analogs of the extended Au-(1×1) and Au-(1×3) structures described here. In the arrangement of the (1×3) surface, all the first-layer atoms of the bilayer Au structure are accessible to the reactants, a morphology that may very well contribute to its exceptional catalytic activity.

Recent density functional theoretical calculations have shown that O_2 adsorbs preferentially and readily dissociates at the Au-TiO_2 interface (*32*). However, as we noted earlier, for the Au-(1×3) structure, access by O_2 to the Au and Ti interface is precluded. In any case, if O_2 activation is promoted by the Au-(1×1) sites and CO adsorbs on the Au-(1×3) sites, theory predicts a relatively small barrier for the CO-O_2 reaction (*33*).

References and Notes

1. M. Haruta, N. Yamada, T. Kobayashi, S. Ijima, *J. Catal.* **115**, 301 (1989).
2. M. Valden, X. Lai, D. W. Goodman, *Science* **281**, 1647 (1998).
3. D. W. Goodman, *J. Catal.* **216**, 213 (2003).
4. C. Chusuei, X. Lai, K. Luo, Q. Guo, D. W. Goodman, *Top. Catal.* **14**, 71 (2001).
5. D. C. Meier, D. W. Goodman, *J. Am. Chem. Soc.* **126**, 1892 (2004).
6. V. A. Bondzie, S. C. Parker, C. T. Campbell, *Catal. Lett.* **63**, 143 (1999).
7. M. Haruta, *CATTECH* **6**, 102 (2002).
8. J. J. Pietron, R. M. Stroud, D. R. Rolison, *Nano Lett.* **2**, 545 (2002).
9. J. Guzman, B. C. Gates, *J. Am. Chem. Soc.* **126**, 2672 (2004).
10. M. M. Schubert *et al.*, *J. Catal.* **197**, 113 (2001).
11. A. T. Bell, *Science* **299**, 1688 (2003).
12. N. Lopez *et al.*, *J. Catal.* **223**, 232 (2004).
13. M.-S. Chen, A. K. Santra, D. W. Goodman, *Phys. Rev. B* **69**, 155404 (2004).
14. Materials and methods are available as supporting material on *Science* Online.
15. M.-S. Chen, D. W. Goodman, in preparation.
16. Annealing multilayer Ti_2O_3 or TiO_2 on a Mo(112)-c(2×2)-[SiO_4] surface induces an interface restructuring of the [SiO_4] surface followed by decomposition or desorption at 1200 K.
17. Q. Guo, W. S. Oh, D. W. Goodman, *Surf. Sci.* **437**, 49 (1999).
18. The Mo-O phonon feature is at 78 meV, as deduced from the Mo(112) surface (Fig. 3A, curve a); the comparable feature for Ti_2O_3 is at 88 meV (*17*). A single phonon at 70 meV, corresponding to Ti^{2+}-O-$Pd^{\delta+}$, was observed on a Pd-TiO_x complex (*34*) (fig. S7). This feature for a Ti^{3+}-O-Mo species should appear between 78 and 88 meV.
19. C. Ruggiero, P. Hollins, *Surf. Sci.* **377–379**, 583 (1997).
20. F. Boccuzzi *et al.*, *J. Catal.* **202**, 256 (2001).
21. E. Wahlström *et al.*, *Phys. Rev. Lett.* **90**, 026101 (2003).
22. A. Vijay, G. Mills, H. Metiu, *J. Chem. Phys.* **118**, 6536 (2003).
23. N. Lopez *et al.*, *J. Catal.* **223**, 232 (2004).
24. P. D. Holmes, B. E. Koel, *J. Vac. Sci. Technol. A* **8**, 2585 (1990).
25. D. A. Outka, R. J. Madix, *Surf. Sci.* **179**, 351 (1987).
26. M. Haruta *et al.*, *J. Catal.* **144**, 175 (1993).
27. The factor of 45 is based on a reaction rate for the Au-(1×3) structure of 1.82×10^{-5} mol·s^{-1}·m^{-2} compared to a rate of 4.0×10^{-7} mol·s^{-1}·m^{-2} at comparable reaction conditions for high-surface-area supported Au (*35*).
28. G. C. Bond, D. T. Thompson, *Catal. Rev. Sci. Eng.* **41**, 319 (1999).
29. F. Cosandey, T. E. Madey, *Surf. Rev. Lett.* **8**, 73 (2001).
30. J. A. Rodriguez *et al.*, *J. Am. Chem. Soc.* **124**, 5242 (2002).
31. A. R. Lupini *et al.*, in preparation.
32. Z.-P. Liu, X.-Q. Gong, J. Kohanoff, C. Sanchez, P. Hu, *Phys. Rev. Lett.* **91**, 266102 (2003).
33. L. M. Molina, M. D. Rasmussen, B. Hammer, *J. Chem. Phys.* **120**, 7673 (2004).
34. M.-S. Chen, D. W. Goodman, unpublished data.
35. T. V. Choudhary *et al.*, *J. Catal.* **207**, 247 (2002).

36. We thank Y. Kuroda (Okayama University) for his valuable assistance as a visiting scientist and W. T. Wallace, B. K. Min, K. Gath, E. Ozensoy, C.-W. Yi, Z. Yan, and K. Luo for fruitful discussions, comments, and the supporting data displayed online. Supported by the U.S. Department of Energy, Office of Basic Energy Sciences, Division of Chemical Sciences; the Robert A. Welch Foundation; and the Texas Advanced Technology Program under grant no. 010366-0022-2001.

Supporting Online Material

www.sciencemag.org/cgi/content/full/1102420/DC1
Materials and Methods
Figs. S1 to S7

Accelerated Sea-Level Rise from West Antarctica

R. Thomas,[1,2]* E. Rignot,[2,3] G. Casassa,[2] P. Kanagaratnam,[4] C. Acuña,[2] T. Akins,[4] H. Brecher,[5] E. Frederick,[1] P. Gogineni,[4] W. Krabill,[6] S. Manizade,[1] H. Ramamoorthy,[4] A. Rivera,[2,7] R. Russell,[1] J. Sonntag,[1] R. Swift,[1] J. Yungel,[1] J. Zwally[6]

Recent aircraft and satellite laser altimeter surveys of the Amundsen Sea sector of West Antarctica show that local glaciers are discharging about 250 cubic kilometers of ice per year to the ocean, almost 60% more than is accumulated within their catchment basins. This discharge is sufficient to raise sea level by more than 0.2 millimeters per year. Glacier thinning rates near the coast during 2002–2003 are much larger than those observed during the 1990s. Most of these glaciers flow into floating ice shelves over bedrock up to hundreds of meters deeper than previous estimates, providing exit routes for ice from further inland if ice-sheet collapse is under way.

Perhaps half the present increase in global sea level of ~1.8 mm/year is caused by melting of terrestrial ice (*1*). During the 1990s, nonpolar glaciers accounted for an estimated 0.4 mm/year (*2*) and Greenland for ~0.15 mm/year (*3*). Although data from Antarctica are still sparse, they suggest a net loss from West Antarctica equivalent to ~0.2 mm/year and approximate balance in East Antarctica, where uncertainty remains large (*4*). Substantial grounding line retreat (*5*, *6*), thinning (*7*), and acceleration (*8*) have been observed on glaciers flowing into the Amundsen Sea, with small ice shelves now but larger ones in the past (*9*). These glaciers flow into ice shelves over beds well below sea level, and sustained thinning would allow them to float free from bedrock, potentially easing resistive forces acting on upstream ice

[1]EG&G Inc., NASA Goddard Space Flight Center (GSFC)/Wallops Flight Facility (WFF), Building N-159, Wallops Island, VA 23337, USA. [2]Centro de Estudios Científicos (CECS), Avenida Arturo Prat 514, Casilla 1469, Valdivia, Chile. [3]Jet Propulsion Laboratory (JPL), 4800 Oak Grove Drive, Pasadena, CA 91109, USA. [4]Radar Systems and Remote Sensing Laboratory, University of Kansas, Lawrence, KS 66045, USA. [5]Byrd Polar Research Center, Ohio State University, Columbus, OH 43210, USA. [6]Code 972, NASA-GSFC, Greenbelt, MD 20771, USA. [7]Departamento de Geografía, Universidad de Chile, Casilla 3387, Santiago, Chile.

*To whom correspondence should be addressed. E-mail: thomas@osb.wff.nasa.gov

and thereby leading to further glacier acceleration.

The extent to which ice shelves affect the dynamics of tributary glaciers remains an unresolved controversy within glaciology. Early suggestions that ice-shelf weakening would result in increased discharge from the ice sheet (*10–12*) require ice-shelf "back forces" to affect glacier dynamics over long distances. If correct, this implies that "marine ice sheets" with beds deep below sea level may be vulnerable to rapid collapse if their deep beds extend to the coast and if buttressing ice shelves are removed. But if glacier behavior is determined mainly by local conditions, it is almost immune to distant perturbations (*13*, *14*). The behavior of the Amundsen Sea glaciers, recent acceleration of tributary glaciers soon after ice-shelf breakup along the east side of the Antarctic Peninsula (*15*), and rapid acceleration of Greenland's fastest glacier, Jakobshavn Isbrae, after thinning and breakup of its floating tongue (*16*, *17*) may help to resolve this issue, which is particularly important because it could imply far more rapid ice discharge than currently predicted (*1*) from Antarctica in a warmer climate.

Understanding these observations and predicting future glacier behavior requires detailed measurements of surface elevation and ice thickness, but the remoteness of the Amundsen Sea glaciers limited comprehensive measurements until late 2002, when surveys were made from Punta Arenas by CECS aboard a Chilean Navy P-3 aircraft equipped with NASA sensors, including a conically scanning laser altimeter (*18*) and ice-sounding radar (*19*). Four flights yielded measurements of surface elevations (to ±0.4 m) at a dense array of 2-m laser footprints within a swath ~500 m wide, and ice thickness to ±20 m, along a total flight track of 3500 km. Surveys included Pine Island (PIG), Thwaites (THW), Haynes (HAY), Pope (POP), Smith (SMI), and Kohler (KOH) glaciers (Fig. 1), where our measurements show much deeper bedrock near the coast than had been estimated earlier (*20*). For the flight running mainly close to the coast between PIG and KOH, the bedrock was on average 400 m deeper than previous estimates (Fig. 2), reaching more than 1 km deeper for the SMI and KOH glacier troughs where no data had previously been obtained, with beds up to 2 km below sea level that may connect to the Byrd Subglacial Basin (BSB). Flights over PIG show its northern side to be shallower than earlier estimates, but its main trunk and particularly its southern tributaries are deeper further inland, suggesting another link to the BSB and the potential for ice-sheet collapse if suggestions that marine ice sheets are susceptible to near-coastal perturbations are correct (*10–12*). Using our ice-thickness measurements, together with velocity estimates for 1996 (SMI, HAY, KOH, POP) and 2000 (PIG, THW) derived from interferometric synthetic aperture radar (InSAR), we find that the entire ice-sheet sector [earlier estimates (*4–6*) only addressed individual glaciers] bounded by and including PIG and KOH discharged 253 ± 5 km^3/year of ice at the time of the velocity measurements, compared to a total annual snow accumulation equivalent of 160 ± 16 km^3 of ice over a catchment area of 393,000 km^2 (*21*).

Satellite radar altimetry data show all surveyed glaciers to have thinned rapidly during the 1990s (*5*, *22*), with thinning rates decreasing from ~2, 3, and 5 m/year near PIG, THW, and SMI grounding lines, respectively, to ~0.1 m/year hundreds of kilometers inland. Comparison of our measurements with surface elevations derived from satellite laser altimeter data acquired by NASA's ICESat (*22*, *23*) in late 2003 and early 2004 shows thinning for each of the

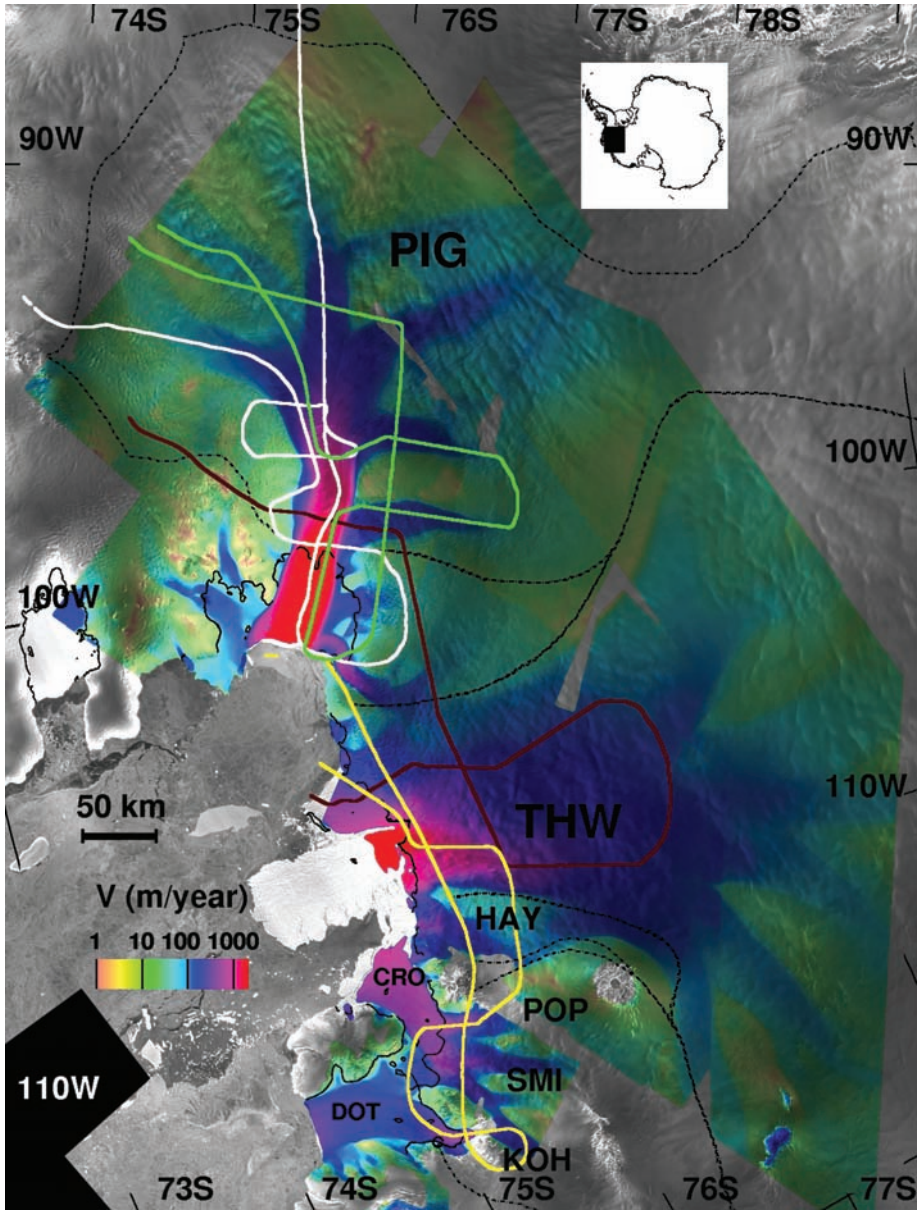

Fig. 1. Part of West Antarctica, showing ice velocities (on a logarithmic scale) derived from 1996 European Remote Sensing Satellites 1 and 2 (ERS-1/2) interferometric radar data (*21*), overlaid on a radar image from Radarsat (*28*). The four CECS/NASA flight lines over Pine Island (PIG), Thwaites (THW), Haynes (HAY), Pope (POP), Smith (SMI), and Kohler (KOH) glaciers, and Crosson (CRO) and Dotson (DOT) ice shelves, are shown in white, brown, yellow, and green lines. Boundaries of catchment basins are marked as thin broken black lines. Grounding line positions in 1996 inferred from ERS-1/2 are shown as thin continuous black lines. Inset shows location in Antarctica.

four flight lines (Fig. 3), with average values ranging from 0.4 m/year (for the flight primarily over PIG tributaries) to 1.8 m/year (for the flight crossing the seaward ends of THW, HAY, POP, SMI, and KOH), and a mean value of 1.0 m/year for all flights. Although the short time interval implies that elevation changes less than a few tens of centimeters per year may simply reflect natural fluctuations in snow accumulation rates, our results show many areas with changes greater than 1 m/year and a pattern of rapid thinning over fast-moving parts of surveyed glaciers. If the 1 m/year average thinning typifies conditions within the ~60,000 km^2 encompassed by our survey, this alone represents a volume loss of ~60 km^3/year from only 15% of the total catchment area. Although this estimate is approximate, it is consistent with losses inferred from mass-budget calculations if average thinning over the rest of the catchment area is 0.1 m/year, as inferred from satellite radar altimetry data (*22*).

Thinning rates near the grounding lines of all surveyed glaciers reach local maxima exceeding 5 m/year, but with high spatial variability resulting from rapid forward motion of the undulating surface. These values are much higher than the earlier estimates, partly because of the smoothing effect of large radar footprints (several kilometers, versus laser footprints of ~2 m for aircraft and 60 m for ICESat), which results in underestimation of high thinning rates along narrow channels occupied by some outlet glaciers, and partly because of a real increase in thinning. Our results from 2002–2003 and 2004 show thinning along the entire main trunk of PIG (Fig. 4A), averaging ~1.2 m/year between 100 and 300 km inland from the grounding line, or double the value from satellite radar altimetry (*24*) for the period 1992–1999 in an area of smoother near-horizontal ice where the radar measurements should give reliable estimates. Further west, flights over THW, SMI, and KOH show rapid thinning within 50 km of the coast (Fig. 4B), decreasing with increasing distance from the sea. This follows a similar pattern to that inferred from satellite radar altimetry (*7*), but with higher thinning rates within 50 km of grounding lines. Further inland, within the THW catchment basin, our results agree with those from radar altimetry data (*7*) indicating little change in thinning rates. This region has surface characteristics very similar to those of inland regions of PIG, where our results show thinning rates approximately double those from earlier radar altimetry data, lending confidence to our conclusion that these measurements show a real increase in thinning rates.

Earlier observations (*25*) showed the seaward 25 km of PIG to be a grounded "ice plain" with surface elevation less than 30 m above flotation elevation. Our 2002 measurements include resurvey of a 1998 airborne survey (*25*), with estimated surface elevation errors of ±0.7 m, and show surface lowering by 20 to 30 m across the ice plain during the 5-year interim. Similar high thinning rates are also shown by comparison of our measurements with those from ICESat along an orbit track that followed our flight line across the ice plain (Fig. 4C). If this continues, most of the ice plain should float free from its bed within the next 5 years.

Flotation of parts of the ice plain may have been responsible for a 9% PIG velocity increase (*8*) between 1996 and 2001 (*26*), representing almost half the 22% increase between 1974 and 2000 (*27*). Here, we compared 24-day repeat data collected by RADARSAT-1 in January–February 2003 and in April 2001, using a speckle-tracking technique, to show that PIG velocity increased another 3.5 ± 0.5% during that time period. This new observation of continued velocity increase is consistent with the increase in thinning rates inferred from our

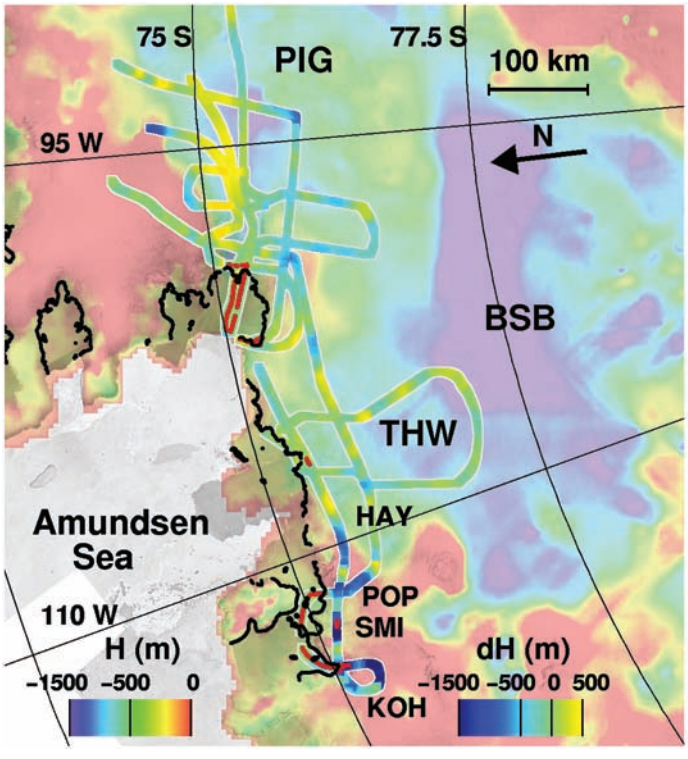

Fig. 2 (left). Bed topography, *H* (*20*), of Amundsen Sea glaciers, omitting elevations above sea level (color scale at lower left), and differences, *dH*, between this and our measurements along flight tracks (color scale at lower right). Sections of floating ice along flight tracks are shown in red. Grounding line positions in 1996 are shown in black. BSB marks the location of the Byrd Subglacial Basin.

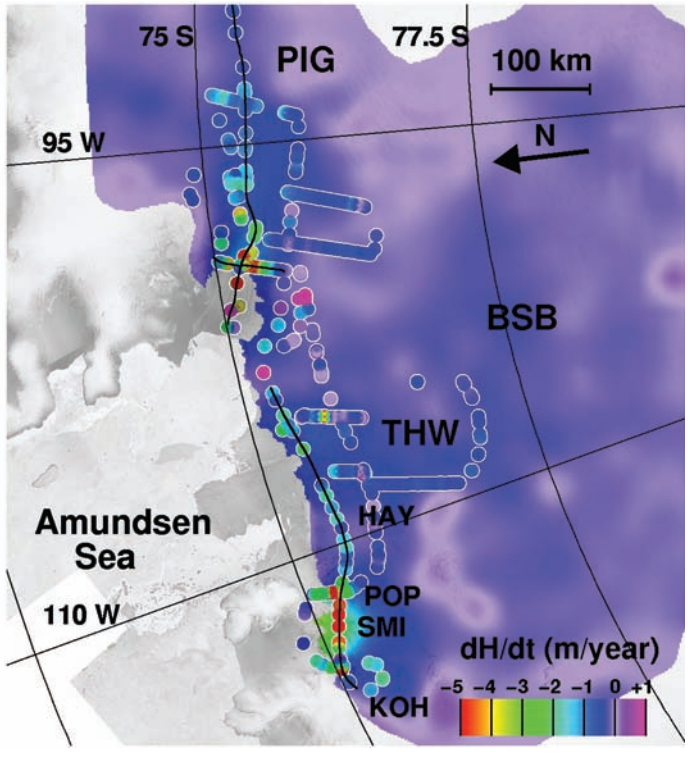

Fig. 3 (right). Thinning rates, *dH*/*dt*, interpolated from ERS-1/2 radar altimetry comparisons (*7*) over Amundsen Sea glaciers, with overlaid values obtained by comparing CECS/NASA airborne and ICESat satellite laser altimetry data. Thin black lines mark locations of profiles shown in Fig. 4.

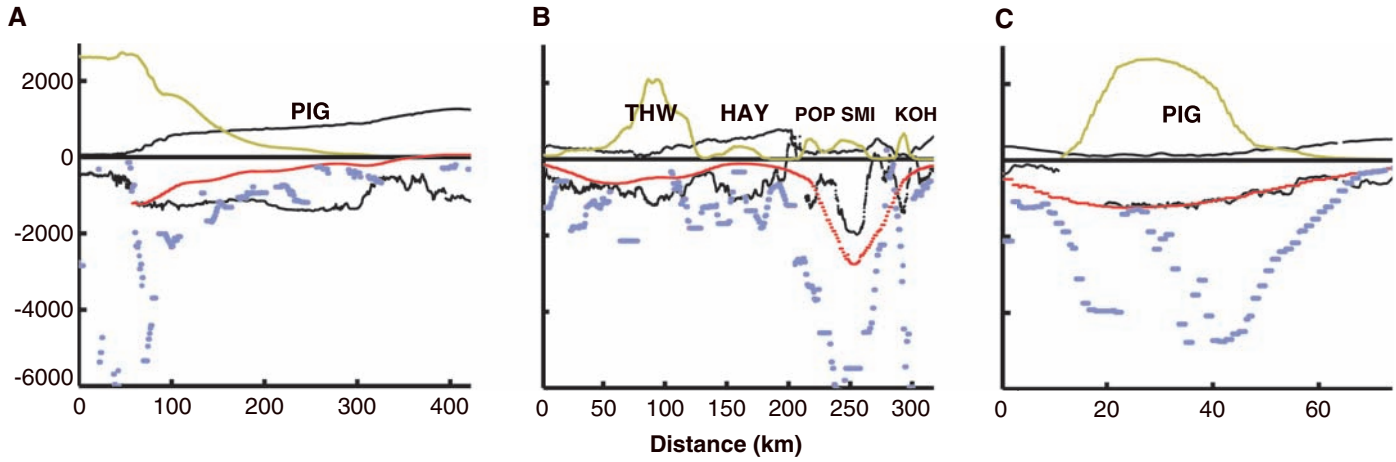

Fig. 4. Surface and bed elevations, shown on the *y* axis in meters (black lines), and rates of elevation change in millimeters per year [red for earlier estimates from ERS-1/2 radar altimetry data (*7*); blue for our results], plotted against distance along sections of flight tracks shown in Fig. 3 for measurements (**A**) along PIG from the ice shelf to the interior; (**B**) along the coast crossing THW, HAY, POP, SMI, and KOH from east to west; and (**C**) across the main trunk of PIG near the grounding line starting from the north. Thinning is largest along the channels of ice discharge occupied by glaciers, as indicated by the ice velocity shown in yellow in meters per year on the *y* axis. High spatial variability in our estimated thinning rates is apparent near the PIG grounding line [(A) and (C)], where down-glacier motion of high-amplitude surface undulations causes excessive local thickening at some locations and thinning at others nearby.

elevation measurements on PIG. Flotation of the entire ice plain is likely to result in further glacier acceleration and additional increases in total ice discharge. The bed of the ice plain deepens from 600 m (below sea level at the grounding line) to 1300 m (25 km further inland) (Fig. 4A). This large thickness slope, together with rapid glacier motion, favors advection thickening by several tens of meters per year as thicker ice moves seaward. Even so, glacier thinning dominates, indicating that thinning by longitudinal stretching exceeds advection thickening. Inland of the ice plain, the bed is almost horizontal for 250 km, and if the grounding line retreats to this deeper region, advection of thicker ice will decrease by an order of magnitude, allowing more rapid thinning. All surveyed glaciers have similar deep beds with ice plains close to flotation in regions more than 10 km upstream from their 1996 grounding-line positions (Fig. 2), making all of them vulnerable to a rapid and widespread response to thickness change.

The catchment regions of Amundsen Sea glaciers contain enough ice to raise sea level by 1.3 m (*6*). Our measurements show them collectively to be 60% out of balance, sufficient to raise sea level by 0.24 mm/year. Although these glaciers are the fastest in Antarctica, they are likely to flow considerably faster once the ice shelves are removed and glacier retreat proceeds into the deeper part of glacier basins.

References and Notes

1. Intergovernmental Panel on Climate Change, *IPCC Third Assessment Report, Climate Change 2001: The Scientific Basis* (Cambridge Univ. Press, Cambridge, 2001).
2. M. Dyurgerov, *Polar Geogr.* **25**, 241 (2001).
3. W. Krabill *et al.*, *Science* **289**, 428 (2000).
4. E. Rignot, R. Thomas, *Science* **297**, 1502 (2002).
5. E. Rignot, *Science* **281**, 549 (1998).
6. E. Rignot, *J. Glaciol.* **47**, 213 (2001).
7. A. Shepherd, D. Wingham, J. Mansley, *Geophys. Res. Lett.* **29** (no. 10), 1364 (2002).
8. E. Rignot, D. Vaughan, M. Schmeltz, T. Dupont, D. MacAyeal, *Ann. Glaciol.* **34**, 189 (2002).
9. T. Kellogg, D. Kellogg, *J. Geophys. Res.* **92**, 8859 (1987) .
10. T. Hughes, *ISCAP Bull.* (Ohio State University), no. 1 (1972).
11. J. Mercer, *Nature* **27**, 321 (1978).
12. R. Thomas, *Geogr. Phys. Quat.* **31**, 347 (1977).
13. P. Huybrechts, *Ann. Glaciol.* **14**, 115 (1990).
14. R. Hindmarsh, *Ann. Glaciol.* **23**, 105 (1993).
15. H. De Angelis, P. Skvarca, *Science* **299**, 1560 (2003).
16. R. Thomas *et al.*, *J. Glaciol.* **49**, 231 (2003).
17. R. Thomas, *J. Glaciol.*, in press.
18. W. Krabill *et al.*, *J. Geodyn.* **34**, 357 (2002).
19. S. Gogineni *et al.*, *J. Geophys. Res.* **106**, 33761 (2001).
20. M. Lythe, D. Vaughan, *J. Geophys. Res.* **106**, 11335 (2001).
21. E. Rignot *et al.*, *Ann. Glaciol.*, in press.
22. J. Zwally *et al.*, *J. Geodyn.* **34**, 405 (2002).
23. NASA's ICESat (Ice, Cloud, and Land Elevation Satellite) was launched into near-polar orbit in February 2003 carrying a laser altimeter (*22*) that operated during February–March and September–November 2003 and during February–March 2004. Some of our aircraft surveys were along ICESat orbits, and all crossed orbit tracks at many locations. Overlapping (by 50%) planar surfaces, or "platelets," were fit to the ~1200 aircraft measurements on each side of the aircraft within a 70-m along-track distance, generally with root-mean-square fit of 10 cm or less. These were compared with ICESat footprint elevations by extrapolating elevations from any platelet within 200 m distance (using the platelet slope), yielding almost 7000 comparisons. The major source of aircraft survey errors was laser pointing, with errors magnified by the 15° off-nadir scan angle. For the ~1000-m altitude flown and a typical maximum roll error of 0.05° (effects of pitch errors are averaged out in the platelet calculation), the resulting elevation error is <0.3 m, with opposite signs on each side of the surveyed swath. Because we averaged about four adjacent ICESat/aircraft comparisons that included data from each side of the aircraft, effects of these roll errors should be largely canceled. Other error sources contribute about ±0.2 m. Accuracy of ICESat measurements is determined mainly by errors in laser pointing and by forward scattering in thin clouds, with the latter edited from the data on the basis of distortion of laser return waveforms. We estimated pointing errors for the September–November 2003 and the 2004 measurements to be <5 arc sec by comparing ICESat data with aircraft surveys over undulating terrain in Antarctica, Greenland, and arid parts of the western United States. Most of our Amundsen glacier surveys were over slopes less than 2°, resulting in slope-induced errors less than ±0.5 m. Consequently, estimated (largely random) errors in elevation changes are less than ±0.6 m. ICESat pointing errors for February–March 2003 data were larger (up to 40 arc sec) and are not included in this analysis.
24. A. Shepherd, D. Wingham, J. Mansley, H. Corr, *Science* **291**, 862 (2001).
25. H. Corr, C. Doake, A. Jenkins, D. Vaughan, *J. Glaciol.* **47**, 51 (2001).
26. R. Thomas, E. Rignot, P. Kanagaratnam, W. Krabill, G. Casassa, *Ann. Glaciol.*, in press.
27. I. Joughin, E. Rignot, C. Rosanova, B. Lucchitta, J. Bohlander, *Geophys. Res. Lett.* **30** (no. 13), 1706 (2003).
28. H. Liu, K. Jezek, B. Li, *J. Geophys. Res.* **104**, 23199 (1999).

29. We dedicate this work to the memory of Niels Gundestrup, who did much to make the project possible despite serious illness. We thank pilots, crew, technicians, and staff from the Armada de Chile, University of Kansas, NASA/WFF, and CECS who helped make the surveys over Antarctica; the British Antarctic Survey, NSF, U.S. Geological Survey, NOAA, Dirección Meteorológica de Chile, and the field team at Base Carvajal for providing weather reports/forecasts and GPS data that made possible the flights and subsequent accurate trajectory calculations; A. Shepherd for estimates of elevation change rates (*7*); NASA's ICESat Project for satellite laser altimeter elevation measurements; and T. Hughes and an anonymous reviewer for suggesting improvements to the paper. Supported by CECS, through Fundación Andes and the Millennium Science Initiative, and by NASA's Cryospheric Processes Program. E.R. performed his work at JPL under a contract with this program.